THE JOURNAL OF BIOLOGICAL CHEMISTRY
Vol. 277, No. 19, Issue of May 10, pp. 17161–17169, 2002
Printed in U.S.A.

Crystal Structure of Binary and Ternary Complexes of Serine Hydroxymethyltransferase from *Bacillus stearothermophilus*

INSIGHTS INTO THE CATALYTIC MECHANISM*

Received for publication, December 15, 2001, and in revised form, February 17, 2002
Published, JBC Papers in Press, February 27, 2002, DOI 10.1074/jbc.M111976200

Vishal Trivedi‡, Amrita Gupta‡, Venkatakrishna R. Jala§, P. Saravanan§, G. S. Jagannatha Rao§, N. Appaji Rao§, Handanahal S. Savithri§, and Hosahalli S. Subramanya‡¶

From the ‡Molecular and Structural Biology Division, Central Drug Research Institute, Chattar Manzil Palace, Mahatma Gandhi Marg, P. B. No. 173, Lucknow 226001, India and §Department of Biochemistry, Indian Institute of Science, Bangalore 560012, India

Serine hydroxymethyltransferase (SHMT), a member of the α-class of pyridoxal phosphate-dependent enzymes, catalyzes the reversible conversion of serine to glycine and tetrahydrofolate to 5,10-methylene tetrahydrofolate. We present here the crystal structures of the native enzyme and its complexes with serine, glycine, glycine, and 5-formyl tetrahydrofolate (FTHF) from *Bacillus stearothermophilus*. The first structure of the serine-bound form of SHMT allows identification of residues involved in serine binding and catalysis. The SHMT-serine complex does not show any significant conformational change compared with the native enzyme, contrary to that expected for a conversion from an "open" to "closed" form of the enzyme. However, the ternary complex with FTHF and glycine shows the reported conformational changes. In contrast to the *Escherichia coli* enzyme, this complex shows asymmetric binding of the FTHF to the two monomers within the dimer in a way similar to the murine SHMT. Comparison of the ternary complex with the native enzyme reveals the structural basis for the conformational change and asymmetric binding of FTHF. The four structures presented here correspond to the various reaction intermediates of the catalytic pathway and provide evidence for a direct displacement mechanism for the hydroxymethyl transfer rather than a retroaldol cleavage.

Serine hydroxymethyltransferase (SHMT;[1] EC 2.1.2.1) is a PLP-dependent enzyme that plays a central role in the one-carbon metabolism. It catalyzes the reversible inter-conversion of serine and tetrahydrofolate to glycine and 5,10-methylene tetrahydrofolate, a key intermediate in the biosynthesis of purine, thymidine, choline, and methionine (1, 2). In addition to this physiological reaction, SHMT has also been shown to catalyze THF-independent aldolytic cleavage, decarboxylation, racemization, and transamination reactions (3). The importance of SHMT in DNA synthesis coupled with the observed high level of enzyme activity in rapidly proliferating cells has focused attention on SHMT as a potential target for the development of anticancer and antimicrobial agents (4–6).

Several mechanisms have been proposed for the hydroxymethyl transfer, the most favored being the retroaldol cleavage (7, 8). The crystal structures of human liver SHMT (hcSHMT) and rabbit liver SHMT (rcSHMT) and *Escherichia coli* SHMT (eSHMT) as well as murine cytoplasmic SHMT (mcSHMT) have been reported (9–12). The structure of a reduced form of rcSHMT representing a *gem* diamine equivalent has also been reported (10). Although these structures have provided a wealth of information regarding the architecture of the enzyme, active site, and residues involved in substrate binding and catalysis, several aspects of SHMT catalytic mechanism remain uncertain (7, 13). A detailed comparison and analysis of several structures of the enzyme corresponding to different intermediate steps and in complex with various substrates, substrate analogs, and product analogs are required to unravel the finer molecular details of the catalytic mechanism. Furthermore, it would be better if these structures could be compared from the same enzyme to eliminate the ambiguities arising from differences in sequence, crystallization conditions, and crystal packing. In this paper we describe and compare the crystal structures of SHMT from *Bacillus stearothermophilus* (bsSHMT) in its internal aldimine form, external aldimine form with bound serine and glycine, and as a ternary complex with glycine and FTHF. Although the structures of the internal aldimine form and ternary complex have been reported earlier (9–12), the external aldimine form with bound serine and glycine are presented in this paper for the first time. A detailed analysis of bsSHMT structures and a comparison with previously reported structures allows an accurate determination of conformational changes in protein structure, orientation of the PLP ring, and key amino acid residues during different stages of catalysis. An analysis of these results provides structural evidence for a direct transfer mechanism for the SHMT catalyzed reaction.

EXPERIMENTAL PROCEDURES

Overexpression and Purification—The SHMT gene was PCR-amplified from *B. stearothermophilus* genomic DNA using the following primers: sense primer, 5′-GGGGGAGCTACATATGAACTACTTGCCAC-3′, and antisense primer, 5′-GAGCGGAAACGGATCCGTCAAAGCGGC-GAC-3′, containing *Nde*I and *Bam*HI restriction sites (underlined nucleotides). The primers were designed using the sequence of SHMT gene from *B. stearothermophilus* available in the data base (GenBank™ accession number E02190). The PCR product was digested with *Nde*I

* This work was supported by the Indian Council of Medical Research, New Delhi, India. This is Central Drug Research Institute communication No. 6249. The costs of publication of this article were defrayed in part by the payment of page charges. This article must therefore be hereby marked "*advertisement*" in accordance with 18 U.S.C. Section 1734 solely to indicate this fact.

The atomic coordinates and structure factors (code 1KKJ, 1KKP, 1KL1, and 1KL2) have been deposited in the Protein Data Bank, Research Collaboratory for Structural Bioinformatics, Rutgers University, New Brunswick, NJ (http://www.rcsb.org/).

¶ To whom correspondence should be addressed. Tel.: 91-522-221411; Fax: 91-522-223405; E-mail: subshs@rediffmail.com.

[1] The abbreviations used are: SHMT, serine hydroxymethyltransferase; bsSHMT, SHMT from *Bacillus stearothermophilus*; rcSHMT, rabbit liver SHMT; eSHMT, *Escherichia coli* SHMT; THF, tetrahydrofolate; FTHF, 5-formyl tetrahydrofolate.

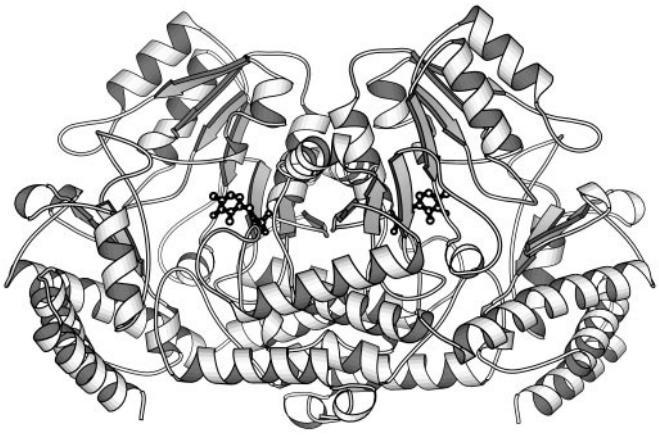

FIG. 1. **The overall fold of the dimer of native bsSHMT, prepared using the program MOLSCRIPT (41).** The cofactor PLP is shown in the *ball* and *stick* representation.

and *Bam*HI and cloned into pRSET C vector at the same sites. The clones were screened by restriction digestion and confirmed by sequencing. The resulting plasmid designated PR bsSHMT was transferred into *E. coli* BL21(DE3) pLysS strain. A single colony was inoculated into 50 ml of LB medium containing 50 μg/ml ampicillin and grown overnight at 30 °C. These cells were used to inoculate 1 liter of terrific broth medium containing 50 μg/ml ampicillin. After 4 h of growth at 30 °C, the cells were induced with 0.3 mM isopropyl-1-thio-β-D-galactopyranoside for 5 h. The isopropyl-1-thio-β-D-galactopyranoside-induced cells were harvested, resuspended in buffer A (50 mM Tris-HCl, pH 7.5, 1 mM EDTA, 1 mM 2-mercaptoethanol), and sonicated. The supernatant was loaded on a MonoQ column equilibrated with buffer A. The protein was eluted using a linear gradient with buffer A containing 1 M NaCl. The fractions containing the protein were pooled and loaded on a phenyl Superose column equilibrated with buffer A containing 1 M ammonium sulfate. The protein was eluted using the same buffer without ammonium sulfate. The fractions containing the protein were pooled and precipitated using ammonium sulfate (65% saturation). The pellet was resuspended in buffer B (100 mM Hepes buffer, pH 7.5, 0.2 mM EDTA, 5 mM 2-mercaptoethanol, 100 mM NaCl) and further purified on a Superdex-200 (Amersham Biosciences) gel filtration column equilibrated with buffer B. Peak fractions corresponding to the dimer were pooled and concentrated to 15 mg/ml using a 50-kDa cutoff Centricon (Amicon).

Crystallization—SHMT protein crystals were grown by hanging drop vapor diffusion method at 25 °C. Protein crystals were obtained by mixing 4 μl of protein solution with 4 μl of reservoir solution containing 100 mM Hepes buffer, pH 7.5, 0.2 mM EDTA, 5 mM 2-mercaptoethanol, 50% 2-methyl-2,4-pentanediol. Crystals started appearing within 4–5 days and grew to a maximum size in 5–10 days. SHMT crystals complexed with serine and glycine were obtained under the same condition as that of the native protein, except that the reservoir solution contained additional 10 mM serine or glycine. The ternary complex crystal of SHMT with glycine and 5-formyl tetrahydrofolate (Sigma) were obtained by adding FTHF to the protein solution (2 mM final concentration) and 10 mM glycine to the reservoir solution. The hanging drops were incubated for 3 h at 18–20 °C and subsequently transferred to room temperature (25 °C).

X-ray Diffraction Data Collection and Processing—Crystals were soaked for a few seconds in a harvesting solution containing 100 mM Hepes buffer, pH 7.5, 0.2 mM EDTA, 5 mM 2-mercaptoethanol, 50% 2-methyl-2,4-pentanediol, and 25% glycerol and flash-frozen in a nitrogen stream (Oxford cryosystems) at 100 K. X-ray diffraction data were collected on a Rigaku Ru-300 x-ray generator using MAR345 image plate detector. The HKL suite was used for data reduction and scaling (14). The native crystals as well as the serine and glycine complex crystals belonged to the space group $P2_12_12$ with one monomer in the asymmetric unit. These crystals diffracted to better than a 2 Å resolution. Final data sets were collected to a 1.93 Å resolution. The ternary complex crystals with glycine and FTHF belonged to the space group $P2_1$ with a dimer in the asymmetric unit and diffracted poorly compared with the native crystals. The final data set was collected to a resolution of 2.7 Å. Details of cell dimensions and data collection statistics for the native and various complex crystals are shown in Table I.

Structure Determination and Model Building—Initially the structure of the internal aldimine form (native form) was determined by molecular replacement technique. A polyalanine model of the structure of *E. coli* SHMT, which shows a sequence identity of 60.8% with the bsSHMT sequence, served as an excellent search model (Protein Data Bank entry 1df0). The final model was composed of residues 5–403 of the *E. coli* structure, modified by omission of residues 243–245 corresponding to insertion in the *E. coli* sequence, based on sequence alignments using CLUSTALW (15). Rotation and translation searches were made using the CCP4 (16) program AMoRe (17). Best solutions were obtained using the data between 10 and 3 Å of resolution. The transformed model was subjected to rigid body refinement using the program XPLOR (18). The N- and C-terminal domains (residues 5–280 and 281–403) of the model were refined independently during rigid body refinement. The phases were improved and extended to 1.93 Å of resolution by solvent flattening using the program DM (19). These phases were used to calculate a $2F_o - F_c$ map and visualized using the graphics program TURBO-FRODO (20). The map was readily interpretable, and the electron density for the PLP cofactor, which was omitted from the model, was clearly visible. Most of the side chains were built into the map, and the model was refined using maximum likelihood positional refinement in REFMAC, with restrained temperature factors (21). After each cycle of refinement, manual rebuilding was performed wherever necessary, and previously undefined side chains were built into the electron density map. The PLP molecule from the eSHMT structure was manually adjusted and built into the electron density map. Solvent molecules were added during final cycles of refinement. The crystallographic free R-factor (22) was monitored at each stage to prevent model bias. The quality of the structure was evaluated using the Ramachandran plot and the program PROCHECK (23). Statistics on the final model are presented in Table I.

The electron density maps for the serine and glycine complex crystals were computed using data to a 1.93 Å resolution from these crystals and refined phases from the native SHMT model without PLP and solvent molecules. The models for the serine- and glycine-bound form were subsequently refined in the same manner as the native form. The model for the ternary form with bound glycine and FTHF was obtained by molecular replacement searches using the native form as the search model. The two monomers in the asymmetric unit were subjected to rigid body refinement before manual model building and subsequent refinement. Strict non-crystallographic symmetry restraints (tight restraints for main chain and medium restraints for the side chain) were applied during refinement. The non-crystallographic symmetry restraints were gradually reduced and completely relaxed during the final round of refinement. Although one of the subunits showed a good electron density for the bound FTHF molecule, the other subunit revealed a much weaker density for the FTHF, and there was no appreciable density for the monoglutamate side chain. Initially the FTHF molecule from the *E. coli* structure was manually adjusted and built into the electron density map for the subunit, showing good density for the bound FTHF. During the final stages of refinement, part of the FTHF molecule (without the monoglutamate side chain) for the other subunit was also included in the model.

Comparison of the bsSHMT structures and earlier reported structures were carried out by manual superposition followed by rigid body refinement option in TURBO-FRODO as well as with the CCP4 program LSQKAB. Differences between the structures were detected visually and by calculating the distances between corresponding Cα atoms. Differences in the orientation of the PLP ring were calculated using the CCP4 program GEOMCALC.

RESULTS

SHMT Structure—The final model of bsSHMT consists of 405 (1–405) residues, including the N-terminal methionine. Seventeen residues were inserted at the C terminus due to the cloning strategy employed. These residues were not visible in the electron density map and, consequently, were not included in the final model. The overall fold of the native enzyme is very similar to that of other known SHMT structures and other PLP-dependent enzymes of the α-class, such as aspartate aminotransferase. Briefly, the monomer fold comprises two major domains, the N-terminal domain (residues 1–279) and a C-terminal domain (280–405). The N-terminal domain can be further divided into two sub-domains, a small N-terminal subdomain (residues 1–80) and a larger PLP binding domain (residues 81–279). The small N-terminal domain comprises three

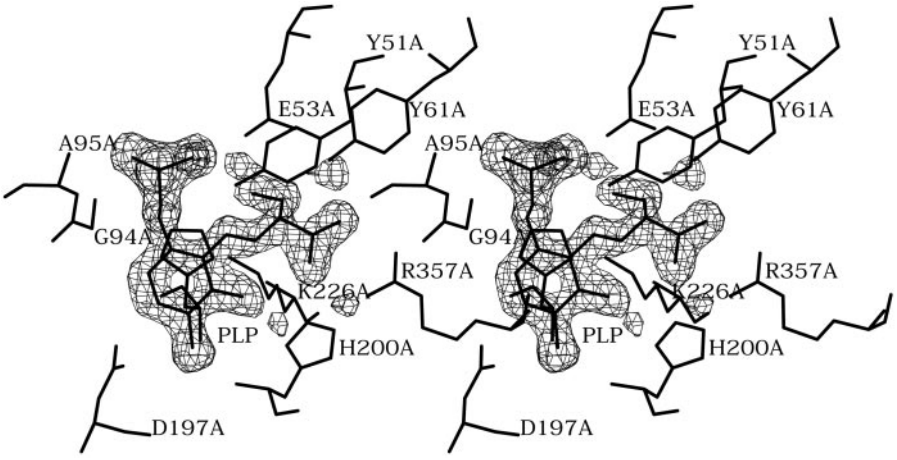

FIG. 2. **Electron density around the cofactor PLP and serine at the active site of bsSHMT serine complex.** The electron density shown is from a $F_o - F_c$ omit map calculated from the final refined phases. Some of the key residues at the active site are shown in stick representation. The figure was prepared using TURBO-FRODO.

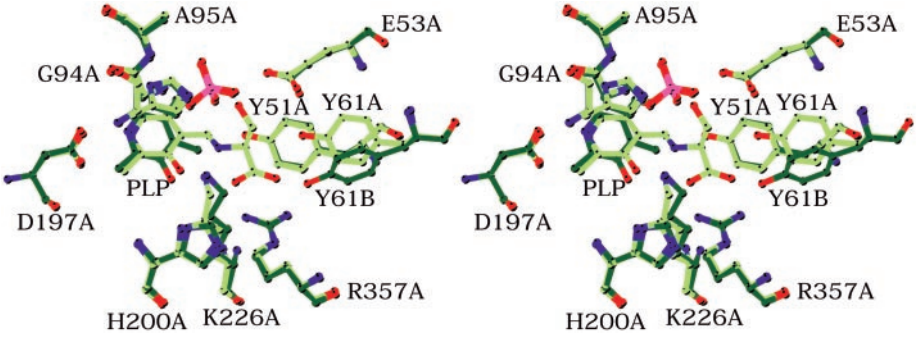

FIG. 3. **Stereoview of the superposition of active site regions in the internal aldimine and external aldimine structures of bsSHMT showing the rotation of the PLP ring and conformational change in the Tyr-61 residue.** The carbon atoms belonging to the internal aldimine and external aldimine structures are shown in *dark green* and *light green* colors, respectively. The nitrogen atoms are shown in *blue*, oxygen atoms are shown in *red*, and phosphorous atoms are shown in *magenta*. The figure was prepared using the program MOLSCRIPT (41).

TABLE I
Statistics for data collection and structure determination

r.m.s.d., root mean square deviation.

	Native	Serine	Glycine	Ternary
Cell dimensions Å	a = 61.15 b = 106.64 c = 56.86	a = 60.98 b = 106.28 c = 56.89	a = 61.27 b = 106.40 c = 56.99	a = 57.42 b = 104.61 c = 62.49 β = 91.43°
Data collection statistics				
Resolution Å	1.93	1.93	1.93	2.70
Completeness (%)	97	96.9	97.6	95.3
Total reflections	68,643	69,596	80,764	53,510
Unique reflections	27,746	27,573	27,979	19,264
R_{sym} %	3.1	3.7	4.3	5.3
Refinement statistics				
Resolution range Å	10–1.93	10–1.93	10–1.93	10–2.70
Final R-factor (all data) (%)	17.86	17.90	16.98	20.84
R_{free} (%)	20.34	20.59	19.73	23.61
r.m.s.d. (bonds) Å	0.009	0.009	0.008	0.009
r.m.s.d. (angles) Å	0.026	0.025	0.025	0.023
Model statistics				
Protein atoms	3,116	3,116	3,116	6,232
Substrate and cofactor atoms	15	22	20	103
Water molecules	226	238	245	57

α-helices and one β-strand, whereas the larger N-terminal domain folds into an $\alpha\beta\alpha$ structure consisting of a seven-stranded mixed β-sheet flanked by α-helices on both sides. The C-terminal domain folds into an $\alpha\beta$ sandwich. All the SHMTs studied to date are either homodimers or homotetramers, the dimer being the minimum structure necessary for the catalytic activity. The four known structures of SHMT (hc-, rc-, mc-, and eSHMT) are all reported to be tetramers, although the quaternary organization of eSHMT structure is different from the mammalian SHMT structures (9–12). In contrast, the quaternary structure of bsSHMT is a dimer. The crystallographic asymmetric unit consists of a monomer, and the two monomers of the dimer are related by the crystallographic symmetry. No tetrameric contacts are visible in the crystal structure. This is consistent with the gel filtration experiments (data not shown), which shows that the protein elutes at a position corresponding to a dimer. The overall structure of the bsSHMT is depicted in Fig. 1.

Serine and Glycine External Aldimine Complexes—The structures of the serine and glycine complexes of bsSHMT are virtually identical to that of the native enzyme except for local conformational changes involving the PLP ring and side-chain atoms in the active site region. When compared with the native structure, the serine and glycine complexes show a root mean

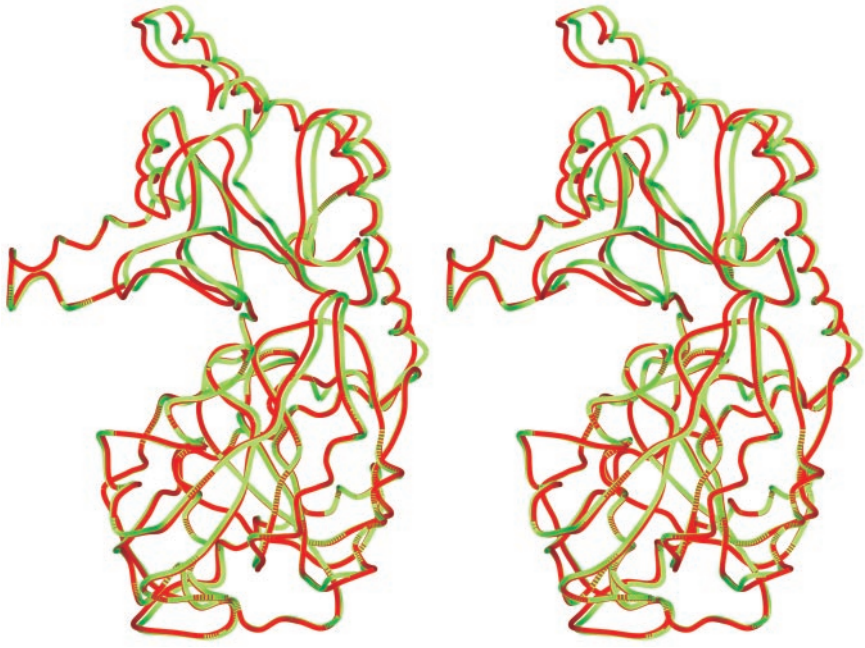

FIG. 4. **Stereoview of the overlaid structures of the monomer A (showing good density for the FTHF) of bsSHMT ternary complex (*red*) and the native structure (*green*) showing differences in the conformations of the C-terminal domain and parts of the N-terminal domain.** The program MOLSCRIPT (41) was used to prepare this figure.

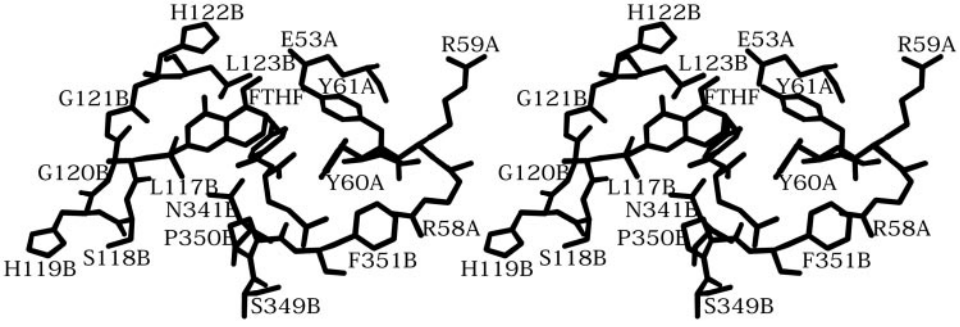

FIG. 5. **Stereoview of the active site region in the monomer A of bsSHMT ternary complex showing the FTHF and key residues interacting with the FTHF molecule.** The figure was prepared using the program MOLSCRIPT (41).

TABLE II
Interactions of the FTHF in the monomer A and monomer B of the ternary complex structure of bsSHMT

FTHF atom	Protein residue	Atom	Monomer A	Monomer B
			Å	*Å*
N1	Asn-341	ND2	3.49	3.64
N2	Leu-117	=O	2.95	3.00
N2	Gly-120	=O	3.18	3.94
N2	Gly-121	=O	2.93	3.37
N3	Gly-121	=O	2.60	2.89
O4	Leu-123	N	2.79	2.88
O5	Glu-53	OE1	2.51	2.87
O5	Glu-53	OE2	2.58	2.61
N8	Asn-341	OD1	2.76	2.99
N10	Glu-53	OE2	3.19	3.37
OE1	Ser-349	OG	3.00	
OE1	Phe-351	N	3.40	
O1	Tyr-60	OH		2.49

square deviation of 0.11 and 0.13 Å, respectively, over the 405 superposed Cα atoms. Several studies have suggested that SHMT undergoes a conformational change upon binding of substrates with a 3-hydroxyl group, resembling the transition that occurs in aspartate aminotransferase from an "open" to "closed" form on binding of the aspartate or 2-methylaspartate substrates (24–26). Thermal stability of the SHMT increases upon binding of serine, and this change in thermal stability of the enzyme has been attributed to a conformational change in SHMT, like that in aspartate aminotransferase (27–30). The crystal structures of mcSHMT and eSHMT complexed to glycine and FTHF indeed show a conformational change compared with the unliganded hc- and rcSHMT structures. However, the observed conformational changes have been largely attributed to the binding of the amino acid substrate (11). The structures of serine and glycine aldimine forms of bsSHMT clearly show that the amino acid substrate binding alone does not induce significant conformational changes in the protein. The conformational changes observed earlier could be a result of FTHF binding. The reported thermal stability of the enzyme is most likely due to the interaction of the serine with the enzyme, particularly those that bridge the two monomers of the dimer, and filling the active site cavity.

The electron density for the bound amino acid substrates was very clear, allowing the substrate to be placed unambiguously. The electron density around the bound serine substrate is shown in Fig. 2. The PLP ring in the serine complex rotates by ~24° (primarily around the C5-C5′ bond) compared with its internal aldimine form (Fig. 3). A similar rotation of the PLP ring has been reported for aspartate aminotransferase (~25°) and between the reduced and unreduced forms of rcSHMT structures (31, 32, 10). In contrast, only a small rotation of the PLP ring (~8°) has been reported in the *E. coli* ternary complex structure relative to the unliganded hc- and rcSHMT structures (11). However, the PLP ring in the *E. coli* structure shows a rotation of about 21° compared with the native form of bsSHMT. The orientation of the PLP is very similar between the two external aldimine forms of the bsSHMT, except for minor movements in the serine complex, to accommodate the

TABLE III
Interactions of the PLP group in the four structures of bsSHMT

PLP atom	Protein residue	Atom	Native	Serine complex	Glycine complex	Ternary complex	
						Monomer A	Monomer B
			Å	*Å*	*Å*	*Å*	
N1	Asp-197	OD2	2.58	2.66	2.63	3.18	2.99
O3	Lys-226	NZ	2.69				
O3	His-200	ND1	3.00	3.20	3.14	3.18	2.94
O3	Ser-172	OG	3.01	2.62	2.60	2.85	2.86
OP1	Ala-95	N	2.85	2.88	2.87	3.03	3.09
OP1	Ser-93	OG	3.58	3.75	3.68	2.93	3.30
OP2	Thy-51B	OH	2.45	2.46	2.48	2.70	2.56
OP2	Gly-257B	N	2.95	2.90	2.95	3.06	3.19
OP3	Gly-94	N	3.09	3.01	3.06	3.23	3.26

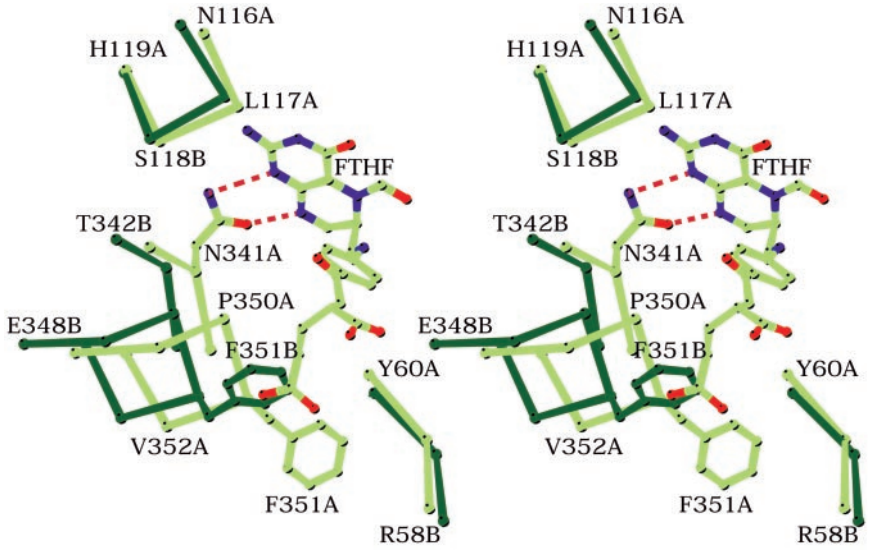

FIG. 6. **The overlaid structures of the native form and the ternary complex (monomer A) of bsSHMT around the monoglutamate binding site.** The difference in the conformations of the loop region (residues 342–352) is depicted. The monoglutamate side chain of FTHF sterically clashes with the Phe-351 residue of the native structure unless this region is moved away from the monoglutamate binding site. The carbon atoms belonging to the native and ternary complex structures are shown in *dark green* and *light green colors*, respectively. The nitrogen atoms are shown in *blue*, and oxygen atoms are shown in *red*. The figure was prepared using the program MOLSCRIPT (41).

additional interactions due to the hydroxyl group of the serine.

The bound serine substrate makes several interactions with both the monomers of the protein. The bound glycine shows exactly the same interactions, except for those formed by the hydroxyl group of the serine. The hydroxyl group of serine is in close proximity of the carboxylate group of GluB53 (2.5 Å). It is also within hydrogen-bonding distance from the imidazole group of HisA122 (2.80 Å). The carboxylate group of serine forms a tight ion pair with ArgA357. In addition, one of the oxygen atoms of the carboxylate group also interacts with the imidazole of HisA200, and the other can form hydrogen bonds with the side chains of SerA31 and TyrB61. An interesting conformational change observed is that of Tyr-61 (Fig. 3). In the native structure, the side chain of TyrB61 is within hydrogen-bonding distance from ArgA357 (2.72 Å), away from GluB53 (5 Å). However, in the serine complex, it flips toward GluB53, away from ArgA357, presumably due to the interaction of the substrate carboxylate group with ArgA357. This conformational change leads to new interaction of TyrB61 with GluB53 and serine carboxylate group and brings the hydroxyl group of TyrB61 close to the Cβ of serine (2.81 Å).

The Ternary Complex—The ternary complex of bsSHMT with bound glycine and FTHF shows small but significant conformational changes compared with the native structure, similar to that observed in the structures of mc- and eSHMT (11, 12). A remarkable feature of the ternary complex structure of bsSHMT is the lack of structural symmetry and differences in the FTHF interaction between the two monomers of the dimer. Although one of the monomers showed a strong density for the FTHF molecule (monomer A), the other monomer revealed a much weaker density, and there was no appreciable density for the monoglutamate part of the molecule in that monomer (monomer B; see "Discussion").

The first clue toward the asymmetry between the two monomers came from the breakdown of orthorhombic symmetry in the crystals of the ternary complex. The crystals of the native and aldimine forms belong to the orthorhombic system with a monomer in the asymmetric unit, whereas the ternary complex crystals belong to the monoclinic system, with a dimer in the asymmetric unit, although the cell dimensions were not very different from the other three forms (Table I). When compared with the native form, both the monomers of the ternary complex show movements in the C-terminal domain (residues 280–405) and parts of the N-terminal domain, particularly around the active site region. The difference between the two monomers of the dimer in the ternary complex appear to be mainly in the extent of these movements. A comparison of the monomer A (showing good density for FTHF) of the bsSHMT ternary complex to the native structure shows a difference of about 4° in the hinge angle between the N- and C-terminal domains, whereas this difference is only 2.5° in the monomer B.

A superposition of the monomer A of the bsSHMT ternary complex with the native structure is shown in Fig. 4. Apart from an overall movement of the C-terminal domain, the ternary complex structure reveals most obvious differences in the region of residues 315–330 and 342–352 of the C-terminal domain and, to a lesser extent, in the regions 27–31 and 114–118 of the N-terminal domain compared with the native structure. Differences in similar regions have been reported in the structures of the ternary complexes of the mc- and eSHMT (11, 12). The carboxylate group of glycine substrate interacts with the hydroxyl group of Ser-31. Furthermore, the region of residues 27–31 is sandwiched between the regions 336–339 and 358–362 of the C-terminal domain. The interaction of Ser-31

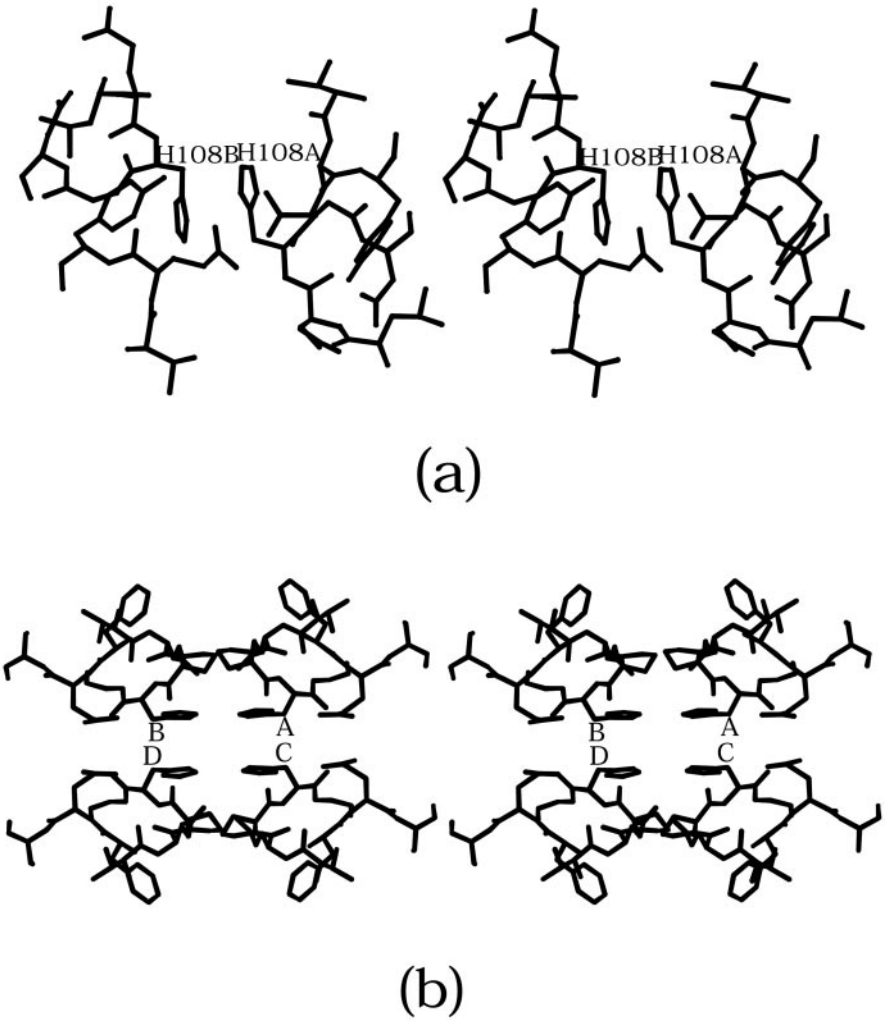

FIG. 7. **Stacking interaction made by His-108 residues in the bsSHMT structure and His-135 residues in the mcSHMT structure.** *a*, stereoview of the region around the His-108 residues at the dimer interface of bsSHMT. *b*, stereoview of the region around the His-135 residues at the tetramer interface of the mcSHMT structure. The His-135 residues in the four subunits are labeled as A, B, C, and D. The figure was prepared using the program MOLSCRIPT (41).

with the carboxylate group of glycine substrate appears to cause a small movement in this region, which is further enhanced by the overall movement of the C-terminal domain. The exocyclic nitrogen of the pteridine ring of FTHF interacts with the main chain carbonyl oxygens of the residues Leu-117, Gly-120, and Gly-121, inducing a small movement in the region 114–119. The position of the loop region 342–352 appears to be important for the FTHF binding. The major difference between the two monomers of bsSHMT appears to be in this loop region. The structural basis for the conformational change in the protein as well as the asymmetric binding of the FTHF will be discussed in the next section.

The bound FTHF molecule is involved in several interactions with the protein. Briefly, the carboxylate group of Glu-53 interacts with the formyl oxygen atom and the N10 atom of the FTHF. The side chain of Asn-341 is within hydrogen-bonding distance from N1 and N8 atoms of the pteridine ring. The C2 amino group of FTHF interacts with the main chain carbonyl oxygen atoms of residues Leu-117, Gly-120, and Gly-121. The main chain carbonyl oxygen of the residue Gly-121 and the amide group of the residue Leu-123 forms hydrogen bonds with the N3 and O4 atoms of FTHF molecule. The *p*-aminobenzoic acid moiety of the FTHF stacks against the side chain of Tyr-60. The monoglutamate part of the molecule makes only one significant interaction with the hydroxyl group of Ser-349 (only in monomer A). A stereo view of the FTHF binding site is shown in Fig. 5, and details of the interactions made by FTHF in both the monomers are presented in Table II. The overall position and orientation of FTHF molecule in bsSHMT is similar to that in the *E. coli* structure. Between the two monomers of bsSHMT, the pteridine ring and the phenyl ring of the FTHF reveal small displacements, and there was no density for the monoglutamate part of the FTHF in the monomer B. The average temperature factor associated with the FTHF in monomer B (~45) was higher when compared with that in monomer A (~37). Furthermore, the interactions of FTHF in monomer B are much weaker compared with those in monomer A (Table II).

PLP Binding Site—Details of interactions made by the PLP in the four structures of bsSHMT are presented in Table III. The overall environment of the PLP, including the interacting protein ligand groups and the ring stacking histidine, is very similar to that found in the known SHMT structures (9–12). It is clear from Table III that these interactions are mostly conserved during different intermediate steps of the catalytic cycle. The interaction of the Nϵ atom of the Lys-226 with the Thr-223 is particularly interesting. The Thr-223 (226 in eSHMT) has been implicated in stabilizing the external aldimine form based on mutational studies (33), which was further confirmed by the crystal structures. In the external aldimine structures of bsSHMT, Lys-226 forms strong hydrogen-bonding interaction with this residue (2.89 Å), similar to that in the eSHMT structure. However, in the ternary complex, this interaction is much weaker, particularly in the monomer B (3.17 Å), and instead, a stronger interaction is made between Lys-226 and TyrB51 (2.8 Å). Tyr-51 appears to play a role in the con-

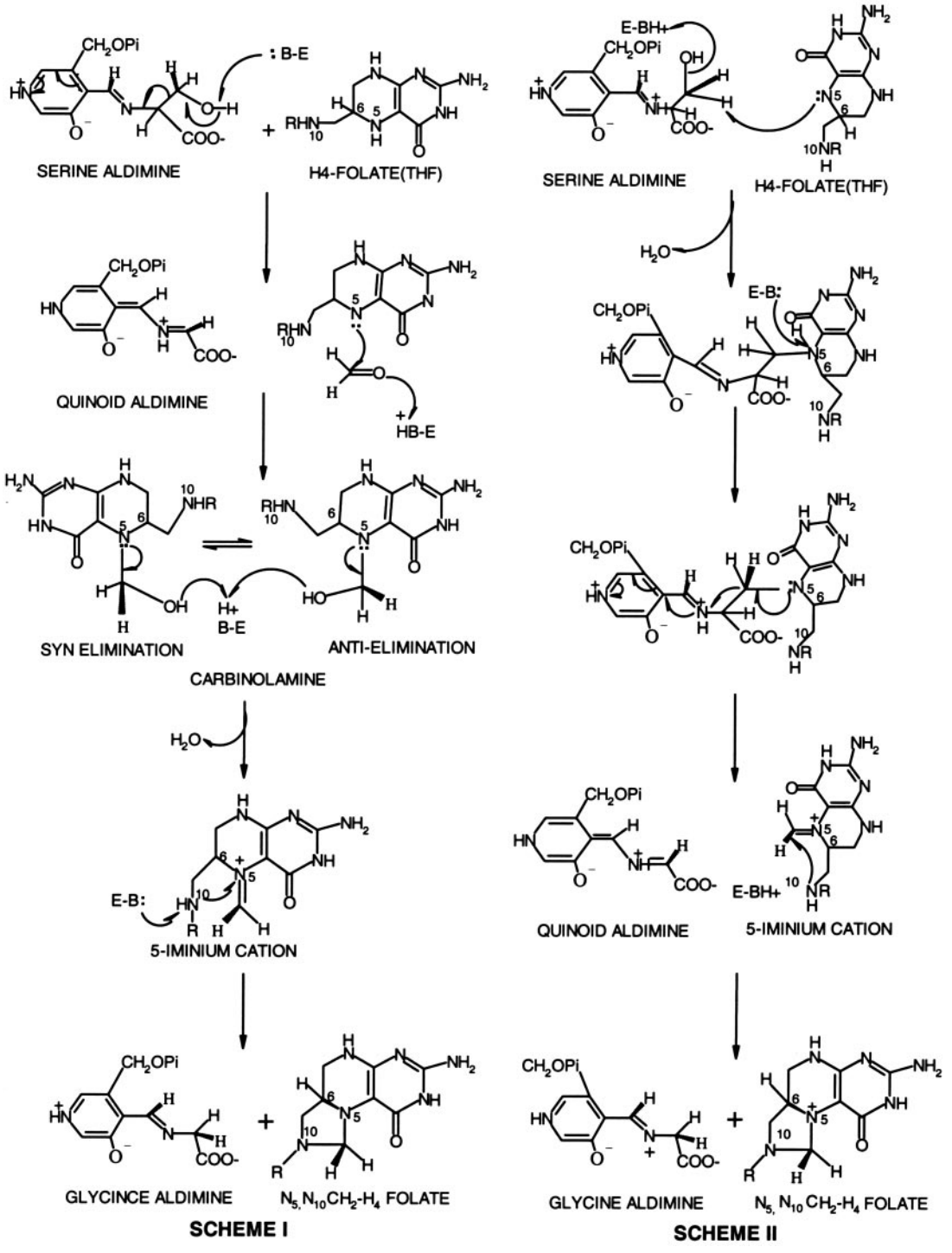

SCHEMES I and II. **Schematic representation of the mechanisms proposed for the reaction catalyzed by SHMT.** I, retroaldol cleavage mechanism; II, direct displacement mechanism.

version of the enzyme from its internal aldimine to the external aldimine form, apart from Thr-223.

DISCUSSION

Structural Basis for the Conformational Changes and Asymmetric Binding of the FTHF—The crystal structures of the ternary complexes of *E. coli*, murine, and bsSHMT clearly establish a small but significant conformational change in the protein compared with the native form, similar to those observed in aspartate aminotransferase (11, 12, 34). In all three structures, the C-terminal domain moves relative to the N-terminal domain, and most obvious differences are observed in the loop region 342–352 (390–400 in mcSHMT, around 350 in eSHMT). The position of this loop appears to be important for the binding of the folate cofactor. Although it was suggested in the mcSHMT structure that the binding of the folate induces a shift in this region, the structural requirement for such a movement was unclear (12). A superposition of the ternary complex of bsSHMT with the native form reveals that the side chain of Phe-351 in the native structure sterically prevents the monoglutamate side chain of the FTHF from binding in that position unless the loop is moved away from that region (Fig. 6). The monoglutamate side chain of the FTHF molecule in the bsSHMT (monomer A) occupies the same position as the side chain of Phe-351 in the native structure, necessitating a move-

ment of this region away from the monoglutamate binding site. The interaction of Asn-341 with N1 and N8 atoms of the pteridine ring appears to facilitate the shift in this loop position.

The spectral and titration calorimetric studies on the rcSHMT have indicated that the ternary complex of the enzyme with glycine and FTHF exists in equilibrium consisting of quinonoid, external aldimine, and *gem* diamine forms (3, 25, 35), which is confirmed by the crystal structure of the mcSHMT (12). In the mcSHMT structure, the two obligate dimers forming the tetramer reveal asymmetric binding of the FTHF, and a loop region (B154-B160) has been implicated in this (12). In contrast, all the active sites of the two dimers in the eSHMT appear to bind glycine and FTHF in a very similar manner (11). The differences in the FTHF binding properties of the murine and *E. coli* SHMT has been attributed to the tetrameric nature of the mammalian enzyme and critical residues in the tetrameric contact region, which are lacking in the *E. coli* enzyme (12). The bsSHMT ternary complex exhibits asymmetric binding of FTHF despite being a dimeric enzyme and lacking the residues corresponding to the loop region 154–160 in the murine structure. The most likely candidate causing the asymmetric binding of FTHF in bsSHMT appears to be the stacking interaction of the imidazole ring of His-108 from the two monomers at the dimer interface of the molecule (Fig. 7). The binding of the folate cofactor results in a small shift in the region 114–119. This movement could be transmitted to the same region of the other subunit via the stacking interaction of the His108 from the two monomers. In other words the displacement in the region 114–119 of the monomer A prevents a similar movement in the monomer B, affecting the binding of FTHF in the monomer B. In the mcSHMT structure, a similar stacking interaction was observed involving His-135 residues (equivalent of His-108) belonging to the two dimers (A-C, B-D) of the tetramer. It is interesting to note that although the asymmetry is found between the two monomers of the dimer of bsSHMT, it is observed between the two obligate dimers of the mcSHMT. In eSHMT on the other hand, which does not exhibit asymmetry in FTHF binding, the residue corresponding to His-108 is a proline (P112), and consequently, no stacking interaction is observed in that structure.

Mechanistic Implications—Several reaction mechanisms have been proposed for the cleavage and transfer of the hydoxymethyl group of serine, the favored mechanism being the retroaldol cleavage (7). The retroaldol cleavage mechanism (Scheme I) requires a catalytic base to abstract a proton from the γ-hydroxyl group of serine and a favorable conformation of the bound substrate for the cleavage reaction to occur. The structure of bsSHMT serine complex reveals two possible candidates for the base, which abstracts a proton from the hydroxyl group of the serine. The side chain carboxylate of Glu-53 and the imidazole group of His-122 (stacking with PLP) are in close proximity of the hydroxyl group of the serine. The side chain carboxylate of Glu-53 has been reported to be in its acid form (protonated), not the conjugated base, in the crystal structure of eSHMT (11). The interaction of Glu-53 in the structure of bsSHMT further confirms this observation. The Glu-53 interacts with 5-formyl oxygen of FTHF in the ternary complex and with immobilized water molecules in the native glycine aldimine as well as in the ternary complex structures of bsSHMT, indicating that it is in its protonated form. Mutation of the equivalent residue in scSHMT (E74Q) has suggested that this residue is not involved in proton abstraction (36). If Glu-53 is in a protonated state, then the only other candidate for the base involved in proton abstraction is His-122. A substantial amount of activity is retained upon mutation of the corresponding residue in sheep liver cytosolic SHMT (H147N), and this residue has been implicated in PLP binding rather than proton abstraction (37). The most favored conformation for this type of cleavage reaction is an antiperiplanar geometry of the atoms involved in electron movement (38). However, the geometry at the Cβ atom of the serine substrate in the external aldimine complex of bsSHMT is not antiperiplanar, instead showing a N-Cα-Cβ-Oγ dihedral angle of 40°, which is not most favorable for the retroaldol cleavage. Thus, the lack of suitable base for proton abstraction as well as the unfavorable conformation of the bound serine suggests the need to consider alternative mechanisms for catalysis more seriously.

The absence of a cysteine residue in close proximity of the active site clearly rules out the possibility of a thiohemiacetal mechanism, which involves nucleophilic attack of a cysteine residue on the β-carbon of the serine. Another possible mechanism is the direct displacement of the Cα bond of the serine aldimine by the phenolate ion of the Tyr-61 residue, leading to the formation of a hemiacetal intermediate. As discussed earlier, Tyr-61 residue undergoes a conformational change upon serine binding and approaches the Cβ atom of the serine (2.8 Å). However, this type of nucleophilic substitution mechanism (S_N2 attack) requires that the nucleophile attacks the carbon atom from the side opposite bond to the leaving group at an angle roughly 180° to the carbon bond of the leaving group (39). The hydroxyl group of Tyr-61 in bsSHMT makes an angle Cα-Cβ-O of 94°, which is orthogonal to the carbon bond of the leaving group and, therefore, not favorable for such a mechanism. Furthermore, mutation analysis of the corresponding residue in the eSHMT as well as sheep liver cytosolic SHMT do not suggest the formation of a hemiacetal intermediate (36, 40). However, the structures of the bsSHMT with serine and ternary complex favors a direct attack of the THF on the serine aldimine (direct displacement mechanism; Scheme II). Assuming no further changes in the position or conformation of the bound serine, a superposition of the serine and ternary complex structures reveals a distance of 2.5 Å between the N5 atom of FTHF and the β-carbon of the serine, optimal for a nucleophilic attack. Furthermore, the angle for nucleophilic attack in this model (as determined by the angle N5-Cβ-Cα) is ~135°. Both the distance and angle are appropriate for a direct attack by the N5 atom of THF at the β-carbon of the serine aldimine. Taken together, these results appear to favor a direct displacement mechanism for the conversion of serine to glycine by SHMT. However, the THF-independent cleavage of other β-hydroxyamino acids could still proceed by a retroaldol cleavage mechanism.

Acknowledgment—We thank Dr. D. K. Dixit for helpful discussions.

REFERENCES

1. Blakely, R. L. (1995) *Biochem. J.* **61,** 315–323
2. Appling, D. R. (1991) *FASEB J.* **5,** 2645–2651
3. Schirch, L. (1984) in *Folates and Proteins: Chemistry and Biochemistry of Folates* (Blakely, R. L., and Benkovic, S. J. eds) pp. 399–412, Wiley Interscience, New York
4. Thorndike, J., Pelliniemi, T. T., and Beck, W. S. (1979) *Cancer Res.* **39,** 3435–3440
5. Eichler, H. G., Hubbard, R., and Snell, K. (1981) *Biosci. Rep.* **1,** 101–106
6. Appaji Rao, N. (1991) in *New Trends in Biological Chemistry* (Ozawa, T., ed) pp. 333–340 Japan Scientific Press, Tokyo
7. Matthews, R. G., and Drummond, J. T. (1990) *Chem. Rev.* **90,** 1275–1290
8. Jordan, P. M., and Akhtar, M. (1970) *Biochem. J.* **247,** 372–379
9. Renwick, S. B., Snell, K., and Baumann, U. (1998) *Structure* (*Lond.*) **6,** 1105–1116
10. Scarsdale, J. N., Kazanina, G., Radaev, S., Schirch, V., and Wright, H. T. (1999) *Biochemistry* **38,** 8347–8358
11. Scarsdale, J. N., Radaev, S., Kazanina, G., Schirch, V., and Wright, H. T. (2000) *J. Mol. Biol.* **296,** 155–168
12. Szebnyi, D. M. E., Liu, X., Kriksunov, I. A., Stover, P. J., and Thiel, D. J. (2000) *Biochemistry* **39,** 13313–13323
13. Matthews, R. G., Drummond, J. T., and Webb, H. K. (1998) *Adv. Enzyme Regul.* **8,** 377–392
14. Otwinowski, Z., and Minor, W. (1997) *Methods Enzymol.* **276,** 307–326
15. Thompson, J. D., Higgins, D. G., and Gibson, T. J. (1994) *Nucleic Acids Res.* **22,** 4673–4680

16. Collaborative Computing Project No. 4 (1994) *Acta Crystallogr. Sect. D Biol. Crystallogr.* **50,** 760–763
17. Navaza, J. (1994) *Acta Crystallogr. Sect. A* **50,** 157–163
18. Brunger, A. T., Karplus, M., and Petsko, G. A. (1989) *Acta Crystallogr. Sect. A* **45,** 50–61
19. Cowtan, K. (1994) *Joint CCP4 and ESF-EACBM Newsletter on Protein Crystallography,* Vol. 31, pp. 34–38
20. Roussel, A., and Cambillau, C. (1989) in *Silicon Graphics Geometry Partner Directory*, pp. 77–78, Silicon Graphics, Mountain View, CA
21. Murshudov, G. N., Vagin, A. A., and Dodson, E. J. (1997) *Acta Crystallogr. Sect. D Biol. Crystallogr.* **53,** 240–245
22. Brunger, A. T. (1992) *Nature* **355,** 472–474
23. Laskowski, R. A., MacArthur, M. W., Moss, D. S., and Thornton J. M. (1993) *J. Appl. Crystallogr.* **26,** 283–291
24. Stover, P., and Schirch, V. (1992) *Biochemistry* **31,** 2155–2164
25. Huang, T., Wang, C., Maras, B., Barra, D., and Schirch, V. (1998) *Biochemistry* **37,** 13536–13542
26. Schirch, V., Shostak, K, Zamora, M., and Gautam-Basak, M. (1991) *J. Biol. Chem.* **266,** 759–764
27. Stover. P., Zamora, M., Shostak, K., Gautam-Basak, M., and Schirch, V. (1992) *J. Biol. Chem.* **267,** 17679–17687
28. McPhalen, C. A., Vincent, M. G., Picot, D., Jansonius, J. N., Lesk, A. M., and Chotia, C. (1992) *J. Mol. Biol.* **227,** 197–213
29. Okamoto, A., Higuchi, T., Hirotsu., Kuramitsu, S., and Kagamiyama, H. (1994) *J. Biochem.* **116,** 95–107
30. Bhaskar, B., Prakash, V., Savithri, H. S., and Rao, N. A. (1994) *Biochim. Biophys. Acta* **1209,** 40–50
31. Jager, J., Moser, M., Sauder, U., and Jansonius, J. N. (1994) *J. Mol. Biol.* **239,** 285–305
32. Arnone, A., Bogers, P. H., Hyde, C. C., Briley, P. D., Mrtzler, C. M., and Metzler, D. E. (1985) in Transaminases (Christen, P., and Metzler, D. E., eds) pp. 138–155, John Wiley & Sons, Inc., New York
33. Angelaccio, S., Pascarella, S., Fattori, E., Bossa, F., Strong, W., and Schirch, V. (1992) *Biochemistry* **31,** 155–162
34. McPhalen, C. A., Vincent, M. G., and Jansonius, J. N. (1992) *J. Mol. Biol.* **225,** 495–517
35. Stover, P., and Schirch,. V. (1991) *J. Biol. Chem.* **266,** 1543–1550
36. Rao, J. V. K., Prakash, V., Rao, N. A., and Savithri, H. S. (2000) *Eur. J. Biochem.* **267,** 5967–5976
37. Jagath, J. R., Sharma, B., Rao, N. A., and Savithri, H. S. (1997) *J. Biol. Chem.* **272,** 24355–24362
38. Gorb, C. A. (1969) *Angew. Chem. Int. Ed. Engl.* **8,** 535–543
39. March, J. (1999) *Advanced Organic Chemistry*, *Reaction*, *Mechanism*, *and Structure*, pp. 294–295, 4th Ed., John Wiley & Sons Ltd. Singapore
40. Contestabile, R., Angelaccio, S., Bossa, F., Wright, T. H., Scarsdale, N., Kazanina, G., and Schirch, V. (2000*) Biochemistry* **39,** 7492–7500
41. Kraulis, P. J. (1991) *J. Appl. Crystallogr.* **24,** 946–950